

Curing Kinetics of Fluorene Containing Benzoxazine Investigated by Nonisothermal Differential Scanning Calorimetry

Yanbing Lu, Mingming Li, Lili Ke, Ding Hu, Weijian Xu

Institute of Polymer Science and Engineering, College of Chemistry and Chemical Engineering, Hunan University, Changsha 410082, China

Received 18 August 2010; accepted 12 December 2010

DOI 10.1002/app.33958

Published online 21 March 2011 in Wiley Online Library (wileyonlinelibrary.com).

ABSTRACT: Fluorene containing benzoxazine monomer (B-pbf) was synthesized from 9, 9-bis(4-hydroxyphenyl) fluorene, aniline, and paraformaldehyde via a solution method. The chemical structure of B-pbf was characterized with FTIR and $^1\text{H-NMR}$. The curing reaction of B-pbf was investigated by nonisothermal differential scanning calorimetry (DSC) at different heating rates. The kinetic parameters and the kinetic models of the curing processes were examined utilizing Kissinger, Ozawa, Flynn-Wall-Ozawa, and Friedman methods. The average activation energy of the curing reaction was determined to be 95.1 kJ

mol^{-1} and 99.0 kJ mol^{-1} , respectively, according to Kissinger and Ozawa method. The autocatalytic kinetic model was found to be the best description of the investigated curing reaction. The reaction order m and n are 0.95 and 2.03, respectively. In addition, the predicted curves from the kinetic models fit well with the nonisothermal DSC thermograms. © 2011 Wiley Periodicals, Inc. *J Appl Polym Sci* 121: 2481–2487, 2011

Key words: benzoxazine; kinetics; fluorene; resins; modeling

INTRODUCTION

Polybenzoxazines, as a class of thermosetting phenolic resins formed by thermal ring-opening of the corresponding benzoxazine monomers without any catalyst, have demonstrated various attractive properties such as high thermal stability, high char yields, high glass transition temperature (T_g), near-zero volumetric change upon curing, good mechanical and dielectric properties, low water absorption, and low flammability.^{1–8} These characteristics make benzoxazine polymers excellent candidates for high performance composites. The wide variety of available phenolic derivatives and primary amines allows for tremendous opportunities in molecular design and imparts the ability to tailor the structure for specific applications.^{9–25}

9,9-Bis (4-hydroxyphenyl) fluorene has a structure of four phenyl rings connected to a quaternary carbon leading to severe rotation hindrance of the phenyl groups.^{26–28} Introduction of the stiff, bulky cardo moieties into benzoxazine can enhance the rigidity and thermal stability of the final product. Although

the effects of chemical structure on the curing and thermal properties of benzoxazine bearing fluorene structure have been studied by Wang et al.,²⁹ there is little information concerning the curing kinetics. The curing kinetic characteristics of a thermoset resin are fundamental to understanding structure–property–processing relationships for the manufacture and utilization of high-performance composites. Such understanding will contribute both to a better knowledge of the process development and to improving the quality of the final products. To understand the nature of curing process of the fluorene containing benzoxazine, benzoxazine monomer bearing fluorene group is synthesized and its curing kinetics is investigated in this work.

EXPERIMENTAL

Materials

The chemicals used and their hazard codes were listed in Table I.

Monomer synthesis

The benzoxazine monomer B-pbf (Scheme 1) was synthesized according to the method reported by Wang et al.²⁹ with some essential modifications.

Paraformaldehyde (12.8 g, 0.16 mol) and 1,4-dioxane (16 mL) were added to a 250-mL three-necked

Correspondence to: Y. Lu (yanbinglu@163.com).

Contract grant sponsor: Natural Science Foundation of Hunan Province, China; contract grant number: 09JJ5009.

TABLE I
Chemicals and Their Hazard Codes

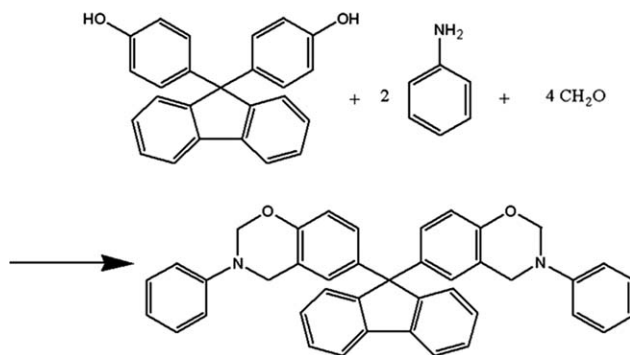
| Chemical | Manufacturer | Hazard code |
|-----------------------------------|---|-------------|
| 9,9-Bis(4-hydroxyphenyl) fluorene | Suqian Ever-Galaxy Pharmacy & Chem. Co | Xi, N |
| Paraformaldehyde | Tianjin Fuchen Chemical Reagent Factory | Xn |
| Aniline | Tianjin Fuchen Chemical Reagent Factory | T, N |
| 1,4-Dioxane | Tianjin Fuchen Chemical Reagent Factory | F, Xn |
| Ethanol | Tianjin Fuchen Chemical Reagent Factory | F |
| Dichloromethane | Tianjin Fuchen Chemical Reagent Factory | Xn |
| Diethyl ether | Tianjin Fuchen Chemical Reagent Factory | F+, Xn |
| Sodium hydrate | Tianjin Fuchen Chemical Reagent Factory | C |

round-bottomed flask equipped with a magnetic stirrer, reflux condenser, and thermometer, stirred 30 min at room temperature. The mixture was cooled to below 5°C in an ice bath, and then aniline (7.48 g, 0.08 mol) was added drop-wise and reacted for 1 h. The temperature was raised gradually to 90°C. A solution of BHPF (14 g, 0.04 mol) in 32 mL mixed solvents including dioxane (16 mL) and ethanol (16 mL) as a cosolvent to improve the solubility of BHPF was added, and the mixture was kept stirring at 90°C for 6 h. The solvent was removed by rotary evaporator. The yellowish powder was dissolved in diethyl ether, washed five times with 3 mol L⁻¹ NaOH aqueous solution and finally two times with distilled water. The ether solution was dried with anhydrous sodium sulfate, filtered, followed by evaporation of ether to afford a yellow crystal. The monomer was further purified by recrystallization from hexane/dichloromethane, dried under vacuum for 2 days. (52% yield).

FTIR (KBr, cm⁻¹): 1232 (C—O—C asymmetric stretching), 1118 (C—N—C asymmetric stretching), 1076 (C—O—C symmetric stretching), 865 (C—N—C symmetric stretching). ¹H-NMR (400 MHz, CDCl₃, ppm): 6.71–7.79 (m, 24H, Ar-H), 5.58 (s, 4H, O—CH₂—N), 4.46 (s, 4H, Ar—CH₂—N).

Characterization

Fourier transform infrared (FTIR) spectrum was performed on a WQF-410 spectrophotometer (Beijing



Scheme 1 Synthesis of B-pbf.

Second Optical Instrument Factory). Proton nuclear magnetic resonance (¹H-NMR) spectrum was recorded on a INOVA-400 instrument (Varian, America).

DSC measurements were carried out on a STA409 differential scanning calorimeter (Netzsch, Germany) at different heating rates (2, 5, 10, 15, and 20°C min⁻¹) in nitrogen atmosphere. Pure indium was used as a standard for calorimetric calibration. The heat flow data, as a function of temperature and time, were obtained by the area under the peak of the exotherm. These data were processed further to obtain the fractional conversion and the rate of curing reaction.

RESULTS AND DISCUSSION

Preparation and characterization of B-pbf

The benzoxazine monomer was prepared from BHPF, aniline, and paraformaldehyde via a solution method. Because of the poor solubility of BHPF in nonpolar solvents such as 1,4-dioxane and/or chloroform, the mixed solvents of 1,4-dioxane, and ethanol were used in the reaction process. Ishida and Low have verified that nonpolar solvents help ring closure of the open Mannich base, and reduce the chances of ring opening.²⁵ In this work, the yield of B-pbf monomers is about 52% while the volume ratio of ethanol and 1,4-dioxane is 1 : 1. The reasons may be attributed to the disadvantageous effect of polar solvent and great steric hindrance of bulky fluorenyl group on the formation of oxazine ring.

The structure of B-pbf was confirmed by FTIR and ¹H-NMR. Figure 1 shows the FTIR spectra of BHPF and the obtained benzoxazine monomer B-pbf. The oxazine ring was observed with the characteristic absorptions at 1232 cm⁻¹ (asymmetric stretching of C—O—C), 1076 cm⁻¹ (symmetric stretching of C—O—C), 1118 cm⁻¹ (asymmetric stretching of C—N—C), and 865 cm⁻¹ (C—N—C symmetric stretching), indicating that monomer containing benzoxazine structure is obtained.^{29–31}

Figure 2 shows the ¹H-NMR spectra of B-pbf and BHPF. The aromatic protons are observed at

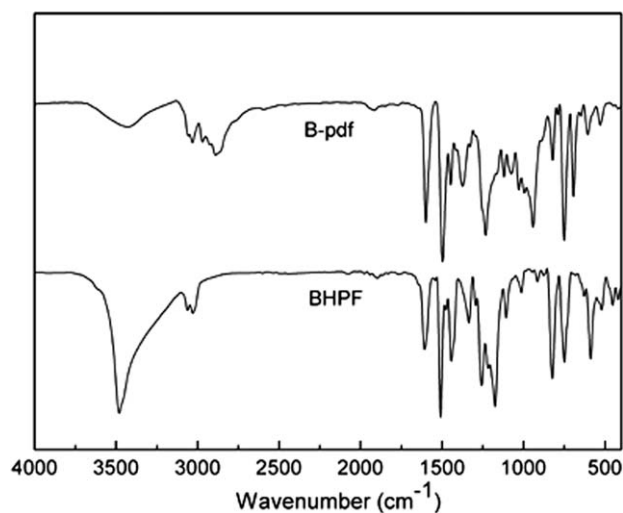


Figure 1 FTIR spectra of BHPF and B-pbf.

6.66–7.79 ppm. Compared with BHPF, the phenolic hydroxyl proton characteristic peak at 9.29 ppm is disappeared in the spectrum of B-pbf. The characteristic peaks appeared at 5.28 and at 4.46 ppm are assigned to methylene (O—CH₂—N) and methylene (Ar—CH₂—C) of the oxazine ring respectively, confirming the formation of benzoxazine monomer.^{29,32–34}

Curing behavior of B-pbf

The curing behavior of the novel fluorine containing benzoxazine B-pbf was studied by DSC. The nonisothermal DSC thermograms at different heating rates are shown in Figure 3. Information about the nature of the curing reaction such as initial curing temperature, peak temperature, and the curing range at different heating rates could be derived. It can be

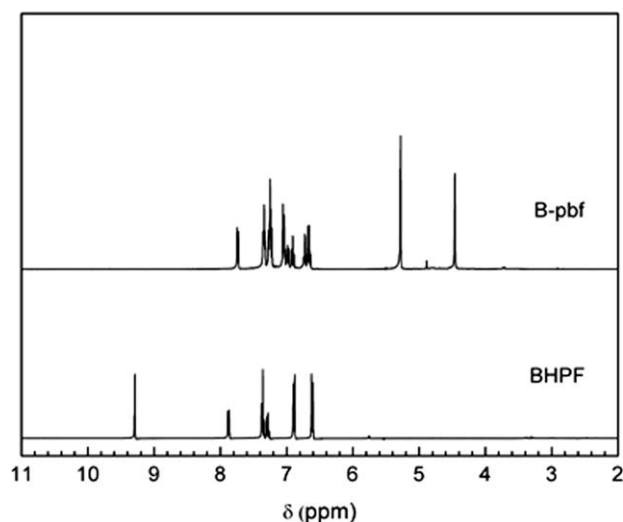


Figure 2 ¹H-NMR spectra of BHPF and benzoxazine B-pbf.

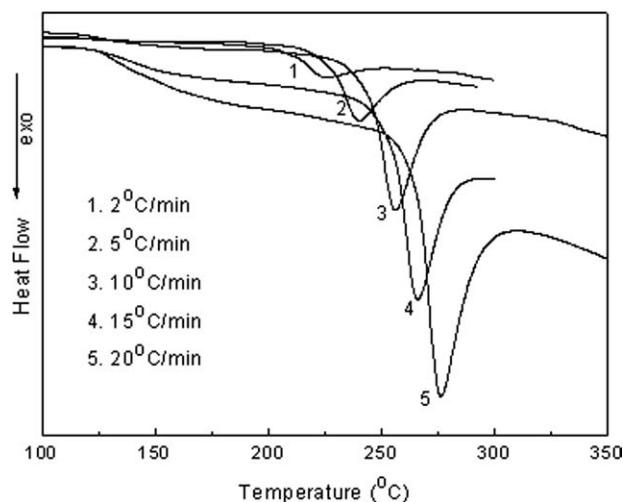


Figure 3 DSC thermograms of B-pbf.

observed that the exothermic peak shifts to higher temperature with higher heating rate.

Kinetic analysis

As for curing kinetics, it is generally assumed that the rate of reaction can be described by two separable functions $K(T)$ and $f(\alpha)$ as follows:

$$d\alpha/dt = K(T)f(\alpha) \quad (1)$$

where $d\alpha/dt$ is the rate of reaction, α the degree of curing reaction, $K(T)$ the temperature-dependent reaction rate constant, and $f(\alpha)$ the function of the degree of reaction. The degree of curing reaction α is given as follows:

$$\alpha = \Delta H_t / H_0 \quad (2)$$

where ΔH_t is the heat released up to a time t and H_0 is the total reaction heat of a reaction.

The temperature dependence of the reaction rate is commonly described by the Arrhenius equation:

$$K(T) = A \exp\left(-\frac{E_a}{RT}\right) \quad (3)$$

where A is the frequency factor, E_a the apparent activation energy, and R the universal gas constant.

For nonisothermal condition, experiments in which samples are heated at a constant rate are conducted. The explicit time dependence can be eliminated so that eq. (1) is represented as follows:

$$\frac{d\alpha}{dT} = \frac{A}{\beta} \exp\left(-\frac{E_a}{RT}\right) f(\alpha) \quad (4)$$

where $\beta = dT/dt$ is the heating rate.

Generally, E_a can be calculated by using three well-known methods for dynamic heating

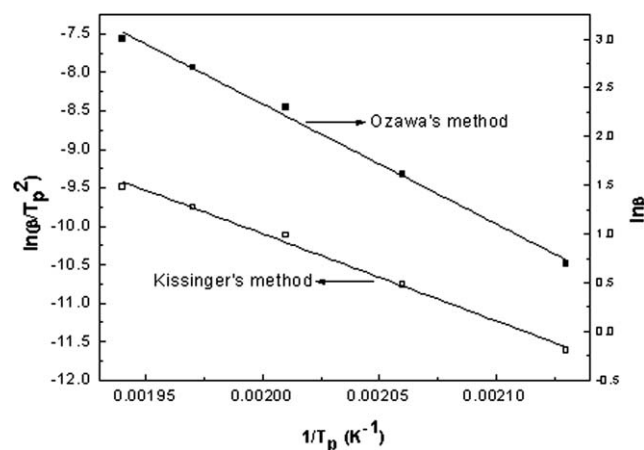


Figure 4 Representations of Kissinger and Ozawa methods to calculation activation energy from nonisothermal data for the benzoxazine monomer.

experiment, Kissinger, Ozawa, and Flynn-Wall-Ozawa method.^{35–37}

Kissinger and Ozawa method

From the heating rate (β) versus reciprocal exothermic peak temperature ($1/T_p$), the activation energy (E_a) of the curing reaction can be calculated by the following two methods, namely, Kissinger method and Ozawa method. Kissinger method is based on the fact that T_p varies with the heating rates and that it assumes the maximum reaction rate ($d\alpha/dt$) occurs at the peak temperatures. The equation can be expressed as eq. (5):

$$\ln(\beta/T_p^2) = \ln(AR/Ea) - Ea/(RT_p) \quad (5)$$

If the plot of $\ln(\beta/T_p^2)$ against $1/T_p$ is linear, the E_a can be obtained from the slope of the corresponding straight line. Figure 4 shows the plot of $\ln(\beta/T_p^2)$ against $1/T_p$ for B-pbf. The E_a value of 95.1 kJ mol^{-1} was estimated using eq. (5).

Another theoretical treatment, namely, the Ozawa method can be also applied to the thermal data, using the following eq. (6):

$$\ln \beta = -5.331 - 1.052 \left(\frac{Ea}{RT_p} \right) + \ln \left(\frac{AEa}{R} \right) - \ln f(\alpha) \quad (6)$$

It is on the assumption that the degree of conversion at peak temperatures for different heating rates is constant. Thus, at the same conversion, the plot of $\ln \beta$ versus $1/T_p$, as shown in Figure 4, should be a straight line with the slope of $1.052 E_a/R$. The E_a value calculated from Figure 4 for B-pbf was 99.0 kJ mol^{-1} . The E_a values from Kissinger and Ozawa methods are quite close to each other and their dif-

ferences may be caused by the different of assumptions.

Flynn-Wall-Ozawa method

Flynn-Wall-Ozawa method is a model-free isoconversional method, which assumes that both the activation energy and pre-exponential factor are functions of the degree of cure. It is based on eqs. (7) and (8).

$$\ln \beta = \ln \left(\frac{AEa}{R} \right) - \ln g(\alpha) - 1.052 \left(\frac{Ea}{RT} \right) - 5.331 \quad (7)$$

$$g(\alpha) = \int_0^\alpha \frac{d\alpha}{f(\alpha)} \quad (8)$$

where $g(\alpha)$ is the integral conversion function.

For a constant α , the plot of $\ln \beta$ versus $1/T$ obtained from DSC thermograms using various heating rates should render a straight line where the slope allows the determination of the apparent activation energy. Figure 5 shows the degree of curing reaction versus the temperature at various heating rates. According to Flynn-Wall-Ozawa method, linear relationships of $\ln \beta$ versus $1/T$ at various degrees were established (Fig. 6), the slope should then correspond to E_a/R at the particular conversion. Figure 7 presents activation energy as a function of curing reaction. It can be seen that the activation energy values tend to increase with the degree of curing reaction. An interpretation of this behavior is an apparent decrease in molecular mobility during the curing process.²⁰

Curing kinetic model

To examine the kinetic model, it requires the previously known activation energy value. In this study, the average activation energy value obtained from

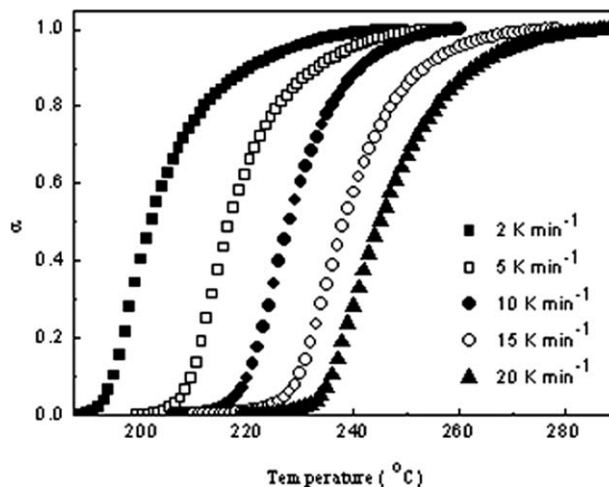


Figure 5 Conversion as a function of cure temperature for B-pbf at different cure rates.

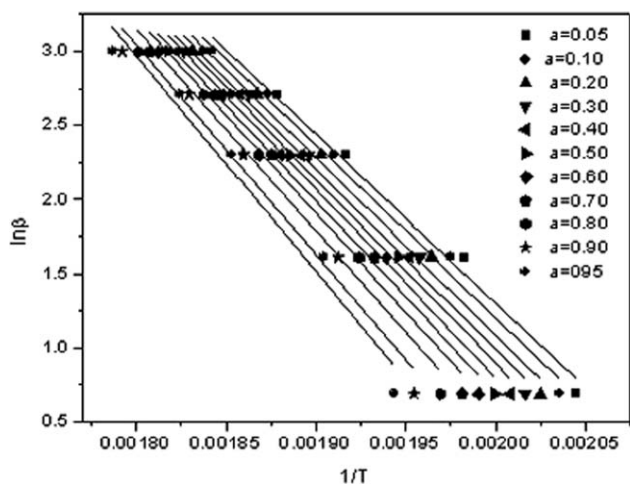


Figure 6 Flynn-Wall-Ozawa plots at various degrees of curing of the benzoxazine resin.

Ozawa’s method was used for the determination of the reaction order of the B-pbf system. In general, the mechanisms of thermoset curing are classified into two major kinetic reactions, an *n*th-order and an autocatalytic reaction.^{27,28} In this work, the method used to find kinetic model is Friedman method.³⁸ This method is based on eq. (9):

$$\ln \frac{d\alpha}{dt} = \ln \beta \frac{d\alpha}{dT} = \ln[Af(\alpha)] - E_a/RT \quad (9)$$

In case of the *n*th-order reaction:

$$f(\alpha) = (1 - \alpha) \quad (10)$$

when *f*(α) in eq. (9) is substituted by eq. (10), eq. (9) could be rewritten as follows:

$$\ln[Af(\alpha)] = \ln \frac{d\alpha}{dt} + E_a/RT = \ln A + n \ln(1 - \alpha) \quad (11)$$

The value of $\ln[Af(\alpha)]$ can be obtained from the known values of $\ln[d\alpha/dt]$ and E_a/RT . Therefore, the

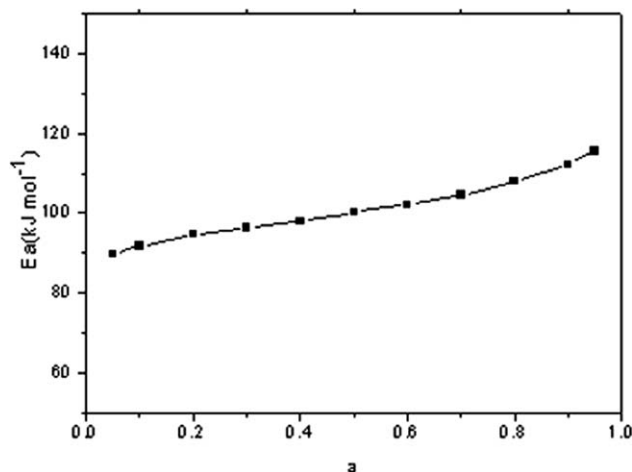


Figure 7 Variation of E_a versus conversion.

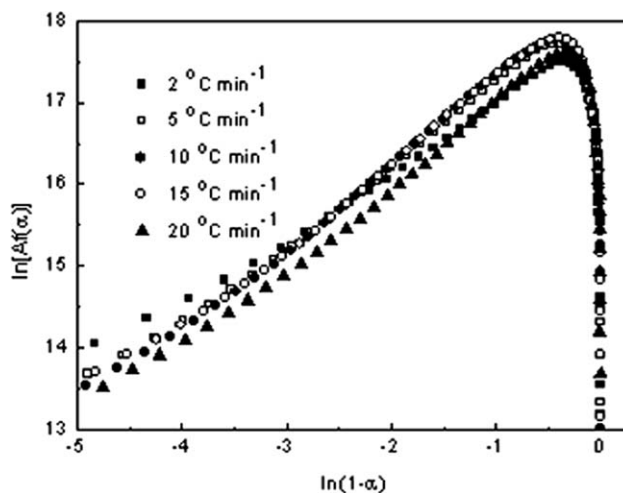


Figure 8 Plots of $\ln[Af(\alpha)]$ versus $\ln(1 - \alpha)$.

plot of $\ln[Af(\alpha)]$ and $\ln(1 - \alpha)$ yields a straight line where the slope corresponds to the reaction order *n*. Otherwise, for autocatalytic process, the Friedman plot would show a maximum of $\ln(1 - \alpha)$ approximately around -0.51 to -0.22 which is equivalent to degree of curing α of about 0.2–0.4. This is due to the autocatalytic nature that shows the maximum reaction rate at 20–40% conversion.

Figure 8 depicts Friedman plots of B-pbf curing reaction at different heating rates. Since $\ln[Af(\alpha)]$ and $\ln(1 - \alpha)$ are not linearly related and evidently show a maximum in the range of the degree of conversion mentioned above, this suggests that the curing reaction is autocatalytic in nature. The autocatalytic nature of benzoxazine resin can be explained by the generation of free phenol groups while the benzoxazine ring open. These groups can actually accelerate further ring opening reaction of the benzoxazine.^{17,22,39}

Owing to the autocatalytic character of the B-pbf system, it was assumed that the reaction could be described by the following general expression for autocatalytic system:

$$f(\alpha) = (1 - \alpha)^n \alpha^m \quad (12)$$

TABLE II
The Kinetic Parameters Evaluated for the Curing Benzoxazine

| Heating Rate (°C min ⁻¹) | E (kJ mol ⁻¹) | $\ln A$ (s ⁻¹) | Mean | <i>n</i> | Mean | <i>m</i> | Mean |
|--------------------------------------|-----------------------------|----------------------------|------|----------|------|----------|------|
| 2 | 99.0 | 19.7 | 19.8 | 2.14 | 2.03 | 0.93 | 0.95 |
| 5 | | 19.7 | | 1.72 | | 0.87 | |
| 10 | | 20.0 | | 1.99 | | 1.02 | |
| 15 | | 20.1 | | 2.15 | | 1.05 | |
| 20 | | 19.7 | | 2.17 | | 0.90 | |

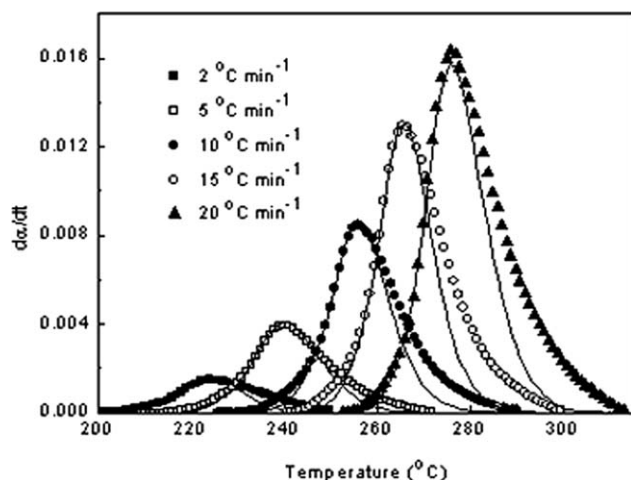


Figure 9 Experimental (symbols) and calculated (solid lines) DSC peaks corresponding to the curing process of benzoxazine monomer.

where m and n are the reaction orders and m describes the autocatalytic character directly.

Substituting eq. (12) into eq. (4), the following expression can be written:

$$\frac{d\alpha}{dT} = \frac{A}{\beta} \exp\left(-\frac{Ea}{RT}\right) (1-\alpha)^n \alpha^m \quad (13)$$

Theoretically, eq. (13) could be solved by multiple nonlinear regressions because the curing rate is an exponential function of the reciprocal of the absolute temperature. By taking the natural logarithm of eq. (13), a linear expression for the natural logarithm of curing rate can be obtained:

$$\ln\left(\beta \frac{d\alpha}{dT}\right) = -\frac{Ea}{RT} + n \ln(1-\alpha) + m \ln(\alpha) + \ln A \quad (14)$$

Equation (14) can be solved by multiple linear regression, in which the dependent variable is $\ln(d\alpha/dt)$, and the independent variables are $1/T$, $\ln(1-\alpha)$ and $\ln(\alpha)$. Therefore, the values of A , m , and n can be obtained using the average activation energy from Ozawa method. The degree of curing is chosen between the beginning of the reaction and the maximum peak of degree of curing ($\alpha = 0.1-0.5$). The results of the multiple linear regressions analysis for all heating rates are listed in Table II.

The experimental curves and predicted curves based on the determined kinetic parameters of curing reaction at different heating rates are shown in Figure 9. It is clearly seen that the calculated data from the model are in good agreement with the experimental results. However, at the later of curing reaction, the mobility of the reaction groups could have been hindered, and the rate of the curing was controlled by diffusion rather than chemical factors.

This may be the reason why the calculated reaction rates are not fit well with the experimental results at this stage.

CONCLUSIONS

9,9-Bis(4-hydroxyphenyl) fluorene based benzoxazine monomer B-pbf was prepared with a solution method and its structure was confirmed by FTIR and $^1\text{H-NMR}$. The curing kinetics of B-pbf was investigated via nonisothermal DSC with Kissinger, Ozawa, Flynn-Wall-Ozawa, and Friedman method. The activation energy by Kissinger and Ozawa method were 95.1 and 99.0 kJ mol^{-1} , respectively. The Flynn-Wall-Ozawa method provided the change of activation energy E_a values as a function of the degree of conversion α . The autocatalytic kinetic model was found to be the best description of the investigated curing reactions. The reaction order m and n are 0.95 and 2.03, respectively. Evidently, the kinetic model of the curing reaction of B-pbf is in good agreement with nonisothermal DSC results.

References

- Ning, X.; Ishida, H. *J Polym Sci Part A: Polym Chem* 1994, 32, 921.
- Ghosh, N. N.; Kiskan, B.; Yagci, Y. *Prog Polym Sci* 2007, 32, 1344.
- Laobuthee, A.; Chirachanchai, S.; Ishida, H.; Tashiro, K. *J Am Chem Soc* 2001, 123, 9947.
- Reghunadhan Nair, C. P. *Prog Polym Sci* 2004, 29, 401.
- Ishida, H.; Allen, D. J. *J Polym Sci Part B: Polym Phys* 1996, 34, 1019.
- Shen, S. B.; Ishida, H. *J Polym Sci Part B: Polym Phys* 1999, 37, 3257.
- Ishida, H.; Sanders, D. P. *Macromolecules* 2000, 33, 8149.
- Zhong, H. L.; Lu, Y. B.; Chen, J. R.; Xu, W. J.; Liu, X. *J Appl Polym Sci* 2010, 118, 705.
- Lin, C. H.; Chang, S. L.; Wei, T. P.; Ding, S. H.; Su, W. C. *Polym Degrad Stab* 2010, 95, 1167.
- Agag, T.; Jin, L.; Ishida, H. *Polymer* 2009, 50, 5940.
- Liu, Y. F.; Yue, Z. Q.; Gao, J. G. *Polymer* 2010, 51, 3722.
- Huang, J. X.; Zhang, J.; Wang, F.; Huang, F. R.; Du, L. *React Funct Polym* 2006, 66, 1395.
- Allen, D. J.; Ishida, H. *Polymer* 2009, 50, 613.
- Tiptipakorn, S.; Damrongsakul, S.; Ando, S.; Hemvichian, K.; Rimdusit, S. *Polym Degrad Stab* 2007, 92, 1265.
- Wang, L.; Zheng, S. X. *Polymer* 2010, 51, 1124.
- Ishida, H.; Low, H. Y. *Macromolecules* 1997, 30, 1099.
- Ishida, H.; Rodriguez, Y. *Polymer* 1995, 36, 3151.
- Rimdusit, R.; Ishida, H. *Polymer* 2000, 41, 7941.
- Kim, H. D.; Ishida, H. *Macromolecules* 2003, 36, 8320.
- Jubsilp, C.; Punson, K.; Takeichi, T.; Rimdusit, S. *Polym Degrad Stab* 2010, 95, 918.
- Yei, D. R.; Fu, H. K.; Chen, W. Y.; Chang, F. C. *J Polym Sci Part B: Polym Phys* 2006, 44, 347.
- Santhosh Kumar, K. S.; Reghunadhan Nair, C. P.; Sadhana, R.; Ninan, K. N. *Eur Polym Mater* 2007, 43, 5084.
- Shi, Z. X.; Yu, D. S.; Wang, Y. Z.; Xu, R. W. *J Appl Polym Sci* 2003, 88, 194.
- Jubsilp, C.; Damrongsakku, S.; Takeichi, T.; Rimdusit, S. *Thermochim Acta* 2006, 447, 131.
- Ishida, H.; Low, H. Y. *J Appl Polym Sci* 1998, 69, 2559.

26. Biolley, N.; Grágoire, M.; Pascal, T.; Sillion, B. *Polymer* 1991, 32, 3256.
27. Yang, G. Z.; Wu, M.; Lu, S.; Wang, M.; Liu, T. X.; Huang, W. *Polymer* 2006, 47, 4816.
28. Zhang, Y.; Huang, Z.; Zeng, W. J.; Cao, Y. *Polymer* 2008, 49, 1211.
29. Wang, J.; Wu, M. Q.; Liu, W. B.; Yang, S. W.; Bai, J. W.; Ding, Q. Q.; Li, Y. *Eur Polym Mater* 2010, 46, 354.
30. Dunkers, J.; Ishida, H. *Spectrochim Acta* 1995, 51A, 855.
31. Dunkers, J.; Ishida, H. *Spectrochim Acta* 1995, 51A, 1061.
32. Ishida, H.; Ohba, S. *Polymer* 2005, 46, 5588.
33. Agag, T.; Takeichi, T. *J Polym Sci Part A: Polym Chem* 2006, 44, 1424.
34. Liu, Y. L.; Yu, J. M.; Chou, C. *J Polym Sci Part A: Polym Chem* 2004, 42, 5954.
35. Kissinger, H. E. *Anal Chem* 1957, 29, 1702.
36. Ozawa, T. *J Therm Anal* 1970, 2, 301.
37. Sbirrazzuoli, N.; Girault, Y.; Elegant, L. *Thermochim Acta* 1997, 293, 25.
38. Friedman, H. L. *J Polym Sci Part C: Polym Symp* 1965, 6, 183.
39. Park, B. D.; Riedl, B.; Hsu, E. W.; Shields, J. *Polymer* 1999, 40, 1689.